

the modulation voltage  $V_m$ .

In summary, preliminary observations have demonstrated a nonlinear interaction of an ion-beam-mode, plasma system. The measured amplitude oscillations are found to be consistent with the ion-beam trapping model. The physical implications of the results are as follows: (1) A modulated ion beam can excite large-amplitude coherent oscillations and subsequent trapping of the beam occurs. (2) The beam ions become bunched in space analogous to the nonlinear interactions of an electron beam and plasma.<sup>7</sup> (3) This spatial bunching provides an effective mechanism for the generation of higher harmonics and could be of interest in spreading the wave spectrum and providing effective coupling of energy into plasmas by means of ion beams.

We thank Dr. N. L. Oleson for helpful and rewarding discussions.

\*Work supported in part by the U. S. Atomic Energy Commission and Tampa Electric Company.

<sup>1</sup>J. H. Malmberg and C. B. Wharton, Phys. Rev. Lett.

19, 755 (1967).

<sup>2</sup>T. M. O'Neil, Phys. Fluids **8**, 225 (1965).

<sup>3</sup>L. M. Al'tshul and V. I. Karpman, Zh. Eksp. Teor. Fiz. **49**, 515 (1965) [Sov. Phys. JETP **22**, 361 (1966)].

<sup>4</sup>A. Lee and G. Schmidt, Phys. Fluids **13**, 2564 (1970).

<sup>5</sup>N. Sato, H. Ikezi, N. Takahashi, and Y. Yamashita, Phys. Rev. **183**, 278 (1969).

<sup>6</sup>W. E. Drummond, J. H. Malmberg, T. M. O'Neil, and J. R. Thompson, Phys. Fluids **13**, 2422 (1970).

<sup>7</sup>T. M. O'Neil, J. H. Winfrey, and J. H. Malmberg, Phys. Fluids **14**, 1204 (1971).

<sup>8</sup>J. H. Malmberg and C. B. Wharton, Phys. Fluids **12**, 2600 (1969).

<sup>9</sup>In such multipole devices, the plasma is supported at the edge by strong short-range magnetic fields which are produced by permanent magnets spaced completely around the plasma. This arrangement leads to higher plasma densities at lower neutral pressures and lower discharge currents, and to plasmas which are highly uniform in density. See, for example, R. Limpacher and K. R. MacKenzie, Bull. Amer. Phys. Soc. **16**, 1222 (1971); R. J. Taylor, D. R. Baker, and H. Ikezi, Phys. Rev. Lett. **24**, 206 (1970).

<sup>10</sup>For example, B. D. Fried and A. Y. Wong, Phys. Fluids **9**, 1084 (1966).

<sup>11</sup>R. A. Stern, J. F. Decker, and P. M. Platzman, Phys. Rev. Lett. **32**, 359 (1974).

## Parametrically Induced Nonlinear Wave-Particle Scattering and Plasma Heating near the Lower Hybrid Frequency

R. P. H. Chang

*Bell Laboratories, Murray Hill, New Jersey 07974*

and

M. Porkolab\*

*Plasma Physics Laboratory, Princeton University, Princeton, New Jersey 08540*

(Received 14 February 1974)

Experimental and theoretical studies of a new type of parametric instability involving the excitation of ion quasimodes (due to nonlinear wave-particle scattering) have been carried out when the "pump" frequency is near the lower hybrid frequency. Plasma heating associated with this instability has also been measured.

Most parametric instabilities studied up to date in a plasma have involved the excitation of resonant electron and ion modes by a "pump" rf field.<sup>1</sup> That is, each of the excited modes satisfies a linear dispersion relationship in the absence of the external rf field. In this Letter we report experimental observations of a new type of parametric instability which involves the excitation of lower-hybrid waves and *nonresonant* low-frequency modes (ion quasimodes) when the "pump" rf field is near the lower hybrid frequency.

Physically, the mechanism for instability is quite similar to that which drives the nonlinear Landau growth.<sup>2</sup> We can view the interaction as a scattering of a particle with a photon and a plasmon, in which a photon is absorbed followed by the emission of a plasmon; the particle carries off the difference of the wave energy and momentum. The growth rate of the instability is maximum when the parallel phase velocity (along the confining magnetic field) of the ion quasimode is of the order of the electron thermal velocity.

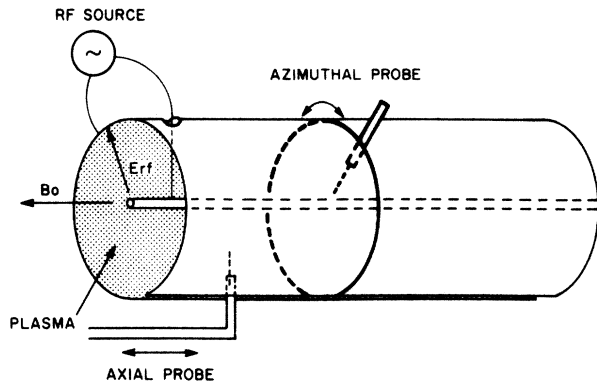


FIG. 1. Simplified schematic of the experimental setup. The pump rf field is applied between the cylindrical shell and the center rod. Waves were measured using the coaxial probes.

Thus, we expect efficient energy transport from the rf field to the bulk of the plasma particles via this nonlinear scattering process. The minimum threshold value for this instability is comparable to that for the purely growing mode, which has been observed recently.<sup>3</sup> In general the nonresonant instability<sup>4</sup> is the dominant one for pump frequencies between 1 to 3 times the lower hybrid frequency [ $1 < \omega_0/\omega_{LH} \lesssim 3$ , where  $\omega_{LH} \equiv \omega_{pi}/(1 + \omega_{pe}^2/\Omega_e^2)^{1/2}$ , with  $\omega_{pj}$  and  $\Omega_j$  being the respective plasma frequency and the gyrofrequency of the  $j$ th species] for  $(M_i/m_e)(k_{||}/k)^2 \approx 1$ ,  $\omega_{pe}/\Omega_e \sim 1$ , and  $T_e \gg T_i$ . Previous theory considered only the resonant decay of ion acoustic modes, and the purely growing instability.<sup>5</sup>

In what follows we shall present experimental results verifying the fundamental aspects of the nonresonant decay instability, and show that substantial plasma heating is associated with the parametrically excited modes. Thus, we believe that these modes will play an important role in future lower-hybrid rf heating of fusion plasmas.

The experiments were performed with the Bell Telephone Laboratories linear plasma device; its properties and plasma parameters have been described previously.<sup>3</sup> In the present experiment the following plasma parameters were used: density,  $N_0 = (1-5) \times 10^{10} \text{ cm}^{-3}$ ; magnetic field,  $B_0 \leq 500 \text{ G}$ ; temperatures,  $T_e = 3-7 \text{ eV}$ ,  $T_i \leq 0.1 \text{ eV}$  for hydrogen and helium gases. A simplified schematic of the experimental setup is shown in Fig. 1. The external rf pump field was coupled to the plasma between a cylindrical shell (radius, 5 cm; length, 100 cm) and a center rod of equal length. A cylindrical geometry was chosen to introduce a pure radial rf pump electric field  $E_{rf}$

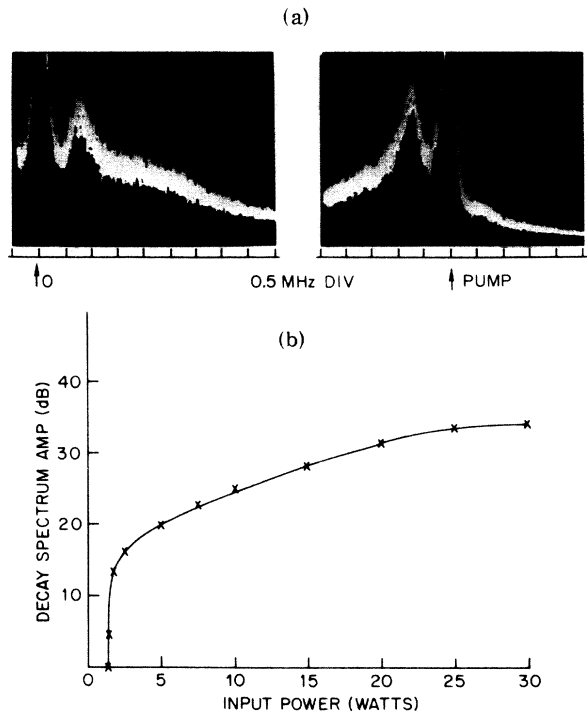


FIG. 2. (a) Decay spectra above threshold for instability. (b) Threshold curve for the most unstable mode in (a).

(which was verified by rf probe measurements). Wavelength and frequency measurements were carried out by means of shielded high-frequency probes shown in Fig. 1.

By coupling to the plasma an rf signal just above the lower hybrid frequency ( $f_0 \approx 30 \text{ MHz}$ ), parametric decay spectra such as shown in Fig. 2(a) were observed above a certain threshold of the pump field. The spectra become broadened with increasing rf power and the rate of increase of the most unstable mode levels off as shown in the threshold curve plot in Fig. 2(b). The threshold drift velocity ( $V_D = CE_{rf}/B_0$ , where  $E_{rf}$  was measured with a calibrated rf probe) was found to be somewhat less than the ion acoustic speed  $V_A$ , in agreement with theoretical predictions.<sup>4</sup> Wavelength measurements (for the most unstable modes) from interferometer traces show the azimuthal mode number,  $m = 2$ , and the parallel wave number,  $k_{||} = 0.03 \text{ cm}^{-1}$ , for both the low-frequency mode and the lower-sideband mode; and  $m = 0$ ,  $k_{||} \approx 0$  for the pump field (for which the skin depth is larger than the plasma diameter).

These measurements show that the wave-number selection rules are satisfied for the para-

metrically excited modes. We note that the low-frequency wave phase velocity along the magnetic field is comparable to the electron thermal velocity  $v_{Te}$ ; thus this mode cannot be an ion acoustic wave (which requires  $\omega/k_{\parallel} \ll v_{Te}$ ). We term the low-frequency modes as ion quasimodes since they are present only in the presence of a pump rf field. The sideband is identified as a lower-hybrid wave,<sup>6</sup>

$$\omega = \omega_{LH} [1 + (k_{\parallel}/k)^2 M_i/m_e]^{1/2},$$

with  $(k_{\parallel}/k)^2 M_i/m_e \simeq 0.5$ . When the pump frequency was raised to 4 or 5 times above the lower hybrid frequency we observed more discrete decay spectra and their higher harmonics. A plot of frequency versus wave number (for this case  $\omega_0 \gg \omega_{LH}$ ) indicated that the low-frequency wave was an ion acoustic wave (i.e.,  $\omega/k_{\parallel} \ll v_{Te}$ ,  $\omega \simeq kv_A$ ) and the lower sideband was a Trivelpiece-Gould mode<sup>7</sup> [ $(k_{\parallel}/k)^2 M_i/m_e \simeq 20$ ]. The observation of these parametrically generated ion acoustic waves has been reported recently.<sup>8</sup>

To study further the ion quasimodes and to compare the results with our theoretical predictions, we have performed a series of test-wave propagation measurements. The experimental setup was the same as that shown in Fig. 1 of Ref. 3. The pump field was coupled to the plasma via a set of parallel plates. To propagate the ion quasimodes in the presence of the pump field, we used a 20-cm-long wire (other lengths were also used) aligned parallel to the magnetic field between the plates as the transmitting wire. Using a movable receiving probe (with a T tip) we have been able to map out the dispersion relationship of the ion quasimode. When the pump frequency was near the lower hybrid frequency,  $\omega_0 \simeq 2\omega_{LH}$ , typical interferometer traces such as those shown in Fig. 3(a) were obtained for the perpendicular wavenumbers ( $k_{\perp} \perp E_{rf} \perp B_0$ ). Parallel wavenumbers were also measured for each corresponding frequency transmitted. The parallel wavenumber increased with decreasing frequency.

A plot of the real part of the dispersion relationship (in circles) is shown in Fig. 3(b). The solid curve is from theory for the corresponding experimental parameters. To check the imaginary part of the dispersion relation for the ion quasimodes, we measured the growth rate of the

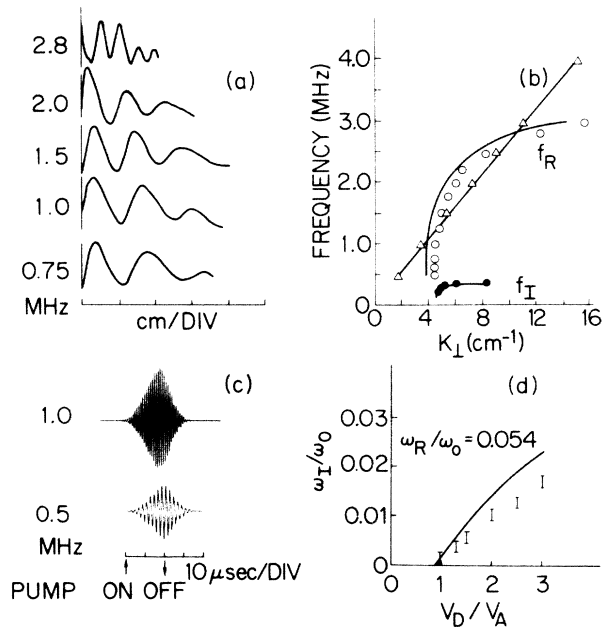


FIG. 3. (a) Interferometer traces of ion quasimodes propagated at different frequencies. (b) Dispersion curves of the ion quasimode (circles and dots) and the ion acoustic mode (triangles); solid curves, theory. (c) Typical ion quasimode oscillation amplitudes after switching on the pump rf field. (d) Growth rate of the ion quasimode as a function of the rf drift velocity  $v_D$  for a fixed frequency. Solid curve, theory.

test wave by pulsing the rf pump field. A rf switch with a typical rise time of 10 nsec was used to turn the pump on and off. Typical oscillograms from a receiving probe for different frequencies are shown in Fig. 3(c) which illustrates very well that these quasimodes will propagate only in the presence of a pump field (in accord with the theory). The measured  $e$ -fold growth rates for the different propagating frequencies are plotted (in dots) in Fig. 3(b). In Fig. 3(d) we have plotted the experimentally measured growth rates as a function of the pump field (the solid curve is from theory) for a fixed transmitted frequency. To study the transition from the nonresonant to the resonant region we increased continuously the pump frequency to more than 4 times the lower hybrid frequency. The dispersion curve (in triangles) shown in Fig. 3(b) indicates the presence of ion acoustic waves for  $\omega_0 \simeq 4.5\omega_{LH}$ . We see that within experimental uncertainties, the above measurements are in good agreement with the theoretical predictions.<sup>4</sup>

To correlate the presence of heating with these instabilities, we observed that as the pump field

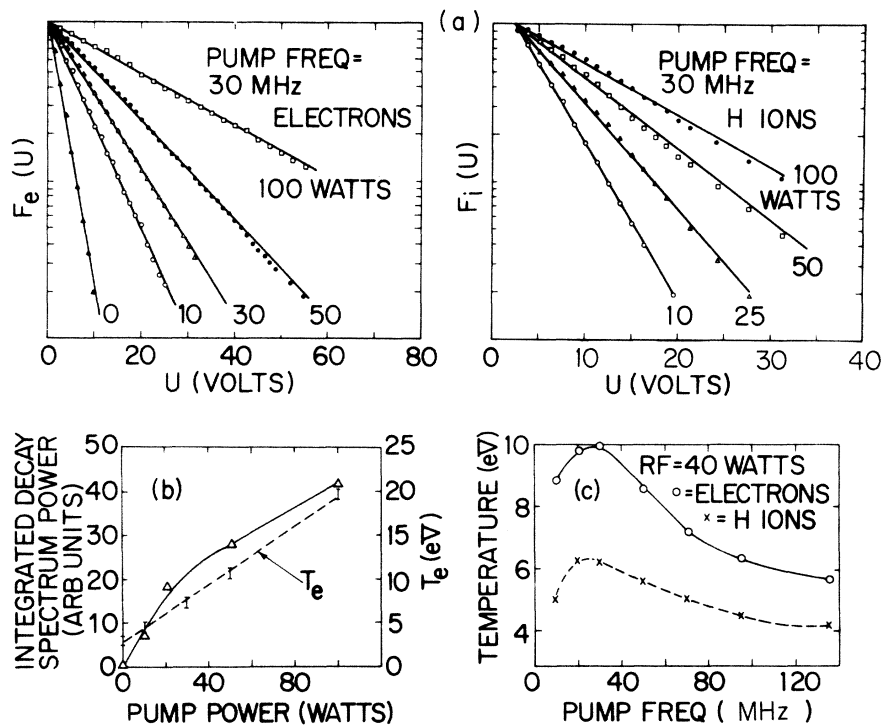


FIG. 4. (a) Electron and ion energy distributions for different pump power near the lower hybrid frequency. (b) Integrated decay wave power (triangles) and electron temperature as functions of the pump power near the lower hybrid frequency. (c) Temperature as a function of the pump frequency for a fixed pump power.

strength was increased, the spectrum became broadened and turbulent (measurements showed that the modes became uncorrelated in a distance less than a wavelength) and at the same time plasma heating took place. The electron temperature was measured by both a Langmuir probe and a shielded multigrid energy analyzer. In addition, a 3-mm-thick shielded multigrid energy analyzer (with the grid surface aligned along the magnetic field lines) was used to measure the perpendicular energy of the ions. The energy distributions of the electrons and ions for different pump powers are plotted in Fig. 4(a). The cutoff for the ions at low energy is due to the finite size of the gyroradius. By plotting the area underneath the decay spectra as a function of the pump power we observe in Fig. 4(b) that the electron temperature increases with increasing wave power.

To substantiate further the fact that the observed heating is due to the presence of the nonresonant instability,<sup>9</sup> we have mapped out heating as a function of the pump frequency for a fixed pump power. From Fig. 4(c), we observe that maximum heating occurs near the lower hybrid frequency ( $f_{LH} \approx 22$  MHz), and that heating occurs

mainly in the regime of nonresonant decay ( $\omega_0/\omega_{LH} \lesssim 3$ ) rather than resonant decay ( $\omega_0/\omega_{LH} > 3$ ).

In conclusion, we have observed a nonresonant decay parametric instability near the lower hybrid frequency. The measured dispersion relationship, growth rates, and thresholds are in good quantitative agreement with our theory. We have also observed the transition from the nonresonant to the resonant decay instability. Furthermore, we have correlated plasma heating with the presence of the nonresonant instabilities. The saturation mechanism, the ion heating mechanism, and the possibility of anomalous plasma transport are now under detailed study.

We thank T. E. Adams for technical assistance and his design of the azimuthal probe. Interest shown by A. Hasegawa, W. L. Brown, and J. A. Giordmaine is appreciated.

\*Work supported in part by the U. S. Atomic Energy Commission under Contract No. AT(11-1)-3073.

<sup>1</sup>A. A. Galeev and R. Z. Sagdeev, Nucl. Fusion **13**,

603 (1973); A. V. Vinogradov *et al.*, *Pis'ma Zh. Eksp. Teor. Fiz.* **17**, 271 (1973) [*JETP Lett.* **17**, 195 (1973)].

<sup>2</sup>R. E. Aamodt and W. E. Drummond, in *Proceedings of the International Conference on Plasma Physics and Controlled Nuclear Fusion Research, Culham, England, 1965* (International Atomic Energy Agency, Vienna, Austria, 1966).

<sup>3</sup>R. P. H. Chang and M. Porkolab, *Phys. Rev. Lett.* **31**, 1241 (1973).

<sup>4</sup>M. Porkolab and R. P. H. Chang, *Bull. Amer. Phys. Soc.* **18**, 1313 (1973); M. Porkolab, Princeton Univer-

sity Report No. MATT 1028 (to be published).

<sup>5</sup>J. M. Kindel, H. Okuda, and J. M. Dawson, *Phys. Rev. Lett.* **29**, 995 (1972).

<sup>6</sup>T. H. Stix, *Phys. Rev. Lett.* **15**, 878 (1965).

<sup>7</sup>A. W. Trivelpiece and R. W. Gould, *J. Appl. Phys.* **30**, 1784 (1959).

<sup>8</sup>W. M. Hooke and S. Bernabei, *Phys. Rev. Lett.* **29**, 1218 (1972); M. Porkolab, V. Arunasalam, and R. A. Ellis, Jr., *Phys. Rev. Lett.* **29**, 1438 (1972).

<sup>9</sup>V. N. Tsytovich, *Usp. Fiz. Nauk* **108**, 143 (1972) [*Sov. Phys. Usp.* **15**, 632 (1973)].

## Turbulent Heating and Quenching of the Ion Sound Instability\*

C. T. Dum, R. Chodura, and D. Biskamp

*Max-Planck-Institut für Plasmaphysik, D 8046 Garching, Germany*

(Received 4 February 1974)

Turbulent heating and stabilization of the ion sound instability is investigated by two-dimensional computer simulation. Quasilinear rather than nonlinear effects determine the evolution of the instability. The instability is quenched by flattening of the electron distribution and the formation of a high-energy ion tail.

Numerous stabilization mechanisms have been proposed for the current-driven ion sound instability.<sup>1-5</sup> We have done extensive simulation studies in order to provide a test for these basic predictions.<sup>6</sup> The two-dimensional code has been described previously.<sup>7</sup> Specifically for the purpose of testing nonlinear theories of stabilization, we have made runs in which the ratio between drift velocity and electron thermal velocity was kept constant, in addition to runs with constant current. In the same vein we discuss the case of a current perpendicular to a weak magnetic field ( $\Omega_e/\omega_e = 0.04$ ). The magnetic field (perpendicular to the plane of computation) has a very small effect on wave dispersion, but keeps the electron distribution isotropic. (In the case of a current along a magnetic field, further complicated dynamical effects are added by the formation of an electron runaway tail.)

We find that for a wide range of initial parameters the growth phase of the instability is followed by the decay of the wave energy  $W$ , the return of the fluctuation level  $W/nT_e$  to the thermal level,<sup>8</sup> and termination of heating in typically  $(100-200)\omega_i^{-1}$ . Clearly, in the case of constant current, the growth phase of the instability must terminate at the latest when the phase velocity reaches the drift velocity,  $u \approx c_s = (T_e/M)^{1/2}$ . The runs with constant  $u/c_s$ , however, show quench-

ing in much the same way; see Fig. 1. It is seen that in this case the plasma enters a regime in which the macroscopic parameters remain constant.

Nonlinear theories of stabilization generally determine a quasisteady fluctuation level  $W/nT_e$  as a function of  $m/M$ ,  $u/v_e$ , and  $T_e/T_i$  from the condition that the nonlinear damping just balances the linear growth rate,  $\gamma = \gamma^L + \gamma^{NL} = 0$ . Actually, for  $(\partial/\partial t) \ln(W/nT_e) = \dot{W}/W - \dot{T}_e/T_e = 0$ ,  $\dot{W}/W \approx 2\gamma$  must be balanced by the electron heat-

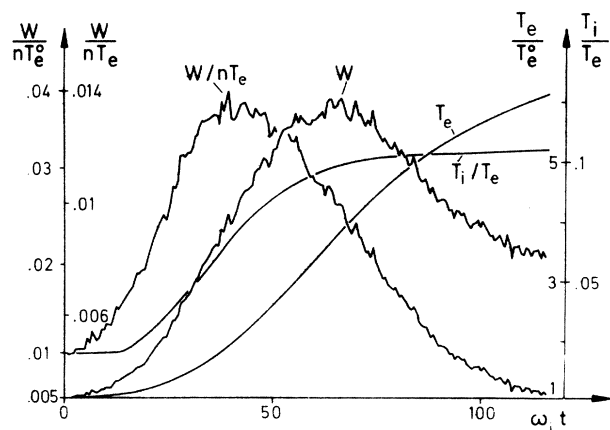


FIG. 1. Wave energy  $W$ , fluctuation level  $W/nT_e$ ,  $T_e$ , and  $T_i/T_e$  for a typical run.  $M/m = 100$ ,  $(T_i/T_e)^0 = 0.02$ ,  $u/v_e = 0.75$ .

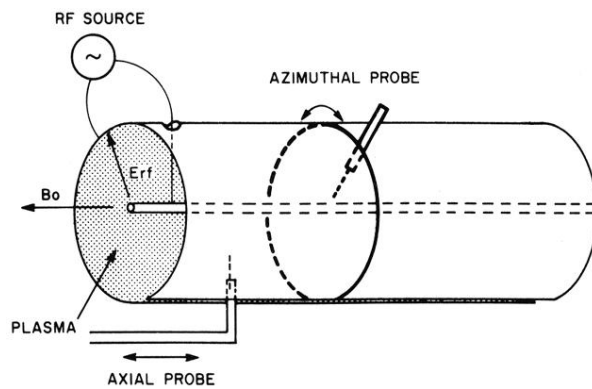


FIG. 1. Simplified schematic of the experimental set-up. The pump rf field is applied between the cylindrical shell and the center rod. Waves were measured using the coaxial probes.

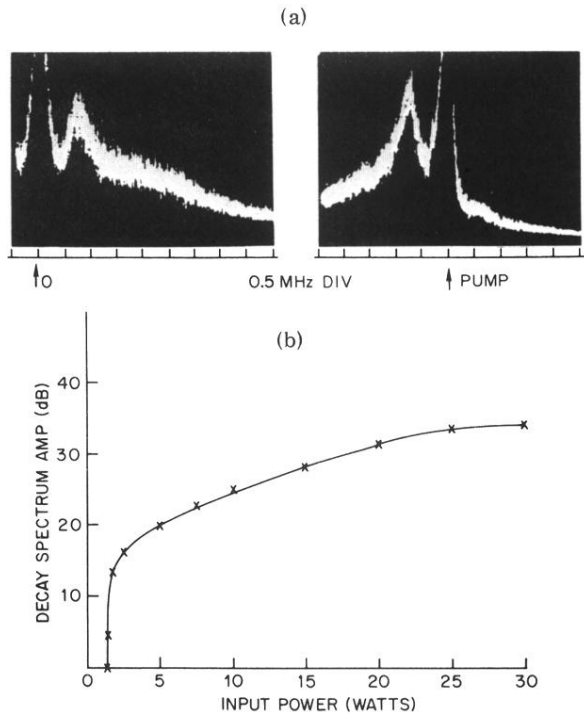


FIG. 2. (a) Decay spectra above threshold for instability. (b) Threshold curve for the most unstable mode in (a).

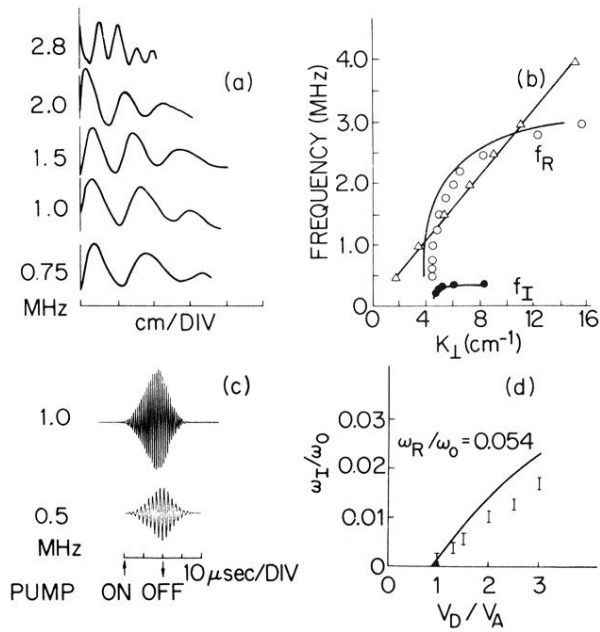


FIG. 3. (a) Interferometer traces of ion quasimodes propagated at different frequencies. (b) Dispersion curves of the ion quasimode (circles and dots) and the ion acoustic mode (triangles); solid curves, theory. (c) Typical ion quasimode oscillation amplitudes after switching on the pump rf field. (d) Growth rate of the ion quasimode as a function of the rf drift velocity  $v_D$  for a fixed frequency. Solid curve, theory.